

Published in final edited form as:

Eur J Nucl Med Mol Imaging. 2009 December ; 36(12): 1987–1993. doi:10.1007/s00259-009-1177-y.

Herpes Simplex Virus Thymidine Kinase Imaging in Mice with (1-(2'-deoxy-2'-[¹⁸F] fluoro-1-β-D-arabinofuranosyl)-5-iodouracil) and metabolite (1-(2'-deoxy-2'-[¹⁸F] fluoro-1-β-D-arabinofuranosyl)-5-uracil)

S Nimmagadda, PhD^{1,2}, TJ Mangner, PhD^{1,3}, JM Lawhorn-Crews, MA^{1,2}, U Haberkorn, MD⁴, and AF Shields, MD PhD^{1,2}

¹ Karmanos Cancer Institute, Wayne State University, Detroit, MI 48201

² Department of Medicine, Wayne State University, Detroit, MI 48201

³ Department of Radiology, Wayne State University, Detroit, MI 48201

⁴ Department of Nuclear Medicine, University of Heidelberg, Germany

Abstract

FIAU, (1-(2'-deoxy-2'-fluoro-1-β-D-arabinofuranosyl)-5-iodouracil) has been used as a substrate for herpes simplex virus thymidine kinases (HSV-TK and HSV-tk, for protein and gene expression respectively) and other bacterial and viral thymidine kinases for noninvasive imaging applications. Previous studies have reported the formation of a de-iodinated metabolite of ¹⁸F-FIAU. This study reports the dynamic tumor uptake, biodistribution and metabolite contribution to the activity of ¹⁸F-FIAU seen in HSV-tk gene expressing tumors and compares the distribution properties with its de-iodinated metabolite ¹⁸F-FAU.

Methods—CD-1 nu/nu mice with subcutaneous MH3924A and MH3924A-stb-tk+ xenografts on opposite flanks were used for the biodistribution and imaging studies. Mice were injected IV with either ¹⁸F-FIAU or ¹⁸F-FAU. Mice underwent dynamic imaging with each tracer for 65 min followed by additional static imaging up to 150 min post injection for some animals. Animals were sacrificed at 60 or 150 min post injection. Samples of blood and tissue were collected for biodistribution and metabolite analysis. Regions of interest were drawn over the images obtained from both tumors to calculate the time activity curves.

Results—Biodistribution and imaging studies showed the highest uptake of ¹⁸F-FIAU in the MH3924A-stb-tk+ tumors. Dynamic imaging studies revealed a continuous accumulation of ¹⁸F-FIAU in HSV-TK expressing tumors over 60 min. The mean biodistribution values (SUV_{±SE}) for MH3924A-stb-tk+ were 2.07_{±0.40}, 6.15_{±1.58}, and that of MH3924A tumors were 0.19_{±0.07}, 0.47_{±0.06} at 60 and 150 min respectively. In ¹⁸F-FIAU injected mice, at 60 min nearly 63% of blood activity was present as its metabolite ¹⁸F-FAU. Imaging and biodistribution studies with ¹⁸F-FAU demonstrated no specific accumulation in MH3924A-stb-tk+ tumors and SUVs for both the tumors were similar to those observed with muscle.

Conclusion—¹⁸F-FIAU shows a continuous accumulation of activity in HSV-TK expressing tumors. ¹⁸F-FAU does not show any preferential accumulation in HSV-TK expressing tumors. In the ¹⁸F-FIAU treated mice, the ¹⁸F-FAU contribution to the total uptake seen in HSV-TK positive tumors is minimal.

Keywords

Fluorine-18; FIAU; HSV-TK; Gene Expression; Metabolism; PET Imaging

Introduction

Fialuridine, [1-(2'-deoxy-2'-fluoro- β -D-arabinofuranosyl)-5-iodouracil; FIAU] is a nucleoside analog and has been investigated as an antiviral agent for Hepatitis B Virus (HBV) infections [1, 2]. FIAU is a preferential substrate to several viral and bacterial thymidine kinases compared to mammalian thymidine kinase. This phenomenon has been utilized to study gene therapy with the reporter gene HSV-tk [3]. FIAU labeled with radiolabeled iodine gained attention as a reporter probe for HSV-TK expression, and vector mediated gene expression has been successfully monitored in patients using ^{124}I -FIAU PET [4]. An overview of the analogs used for gene expression imaging has been briefly reviewed in the literature [5]. Recently, viral thymidine kinase (TK) based accumulation of ^{124}I -FIAU activity has been utilized for the detection of musculoskeletal bacterial infections [6, 7]. These new developments may open up new research avenues for the use of the more clinically favorable agent ^{18}F -FIAU.

Our previous study described the biodistribution and metabolism of ^{18}F -FIAU in normal dogs [8]. ^{18}F -FIAU was metabolized *in vivo* resulting in ^{18}F -FAU. Generation of radioactive metabolites and their contribution to images may complicate the interpretation of results. A clearer understanding of the metabolite contribution to the images, in this particular case possible phosphorylation and trapping of ^{18}F -FAU by HSV-TK, requires further study.

The interest in investigating the substrate specificity of HSV-TK for FAU is two fold. Primarily, to assess ^{18}F -FAU contribution as a metabolite to the ^{18}F -FIAU derived images and secondarily, to further understand the activation of FAU. FAU was developed as an anti-neoplastic agent to take advantage of high thymidylate synthase (TS) levels observed in tumors resistant to 5FU treatment. Once taken up in a cell, it was hypothesized that FAU may be phosphorylated by thymidine kinase to form FAU-monophosphate. Then it will be methylated by TS to FMAU-monophosphate. FMAU-monophosphate will be further phosphorylated by nucleotide kinases and incorporated into DNA [9]. Initial *in vitro* thymidine kinase assay analysis showed FAU to be a poor substrate for mammalian thymidine kinase [10]. This, being a liability, led to exploring the activation of FAU by other nucleoside kinases to improve its therapeutic and/or imaging potential.

To address the substrate specificity of HSV-TK for FAU using a well characterized HSV-tk stably expressing cell line, this study investigated 1) the *in vitro* substrate specificity of HSV-TK for FAU 2) the dynamic uptake and biodistribution of ^{18}F -FIAU and ^{18}F -FAU in mice and 3) the contribution of formed ^{18}F -FAU when ^{18}F -FIAU is used as a gene expression imaging agent.

Materials

^3H -FAU (318.2 GBq/mmol, >99% radiochemical purity), ^{14}C -FIAU (2.0 GBq/mmol, >99% radiochemical purity) were obtained from Moravek Biochemicals (Brea, CA). ^{18}F labeled FIAU and FAU were synthesized as described in the literature using 2,4-bis-O-(trimethylsilyl)-5-iodouracil and 2,4-bis-O-(trimethylsilyl)-uracil as intermediate precursors, respectively [11]. The total synthesis uncorrected yields varied between 10-12% and with specific activity of at least 111GBq/ μmol , purity > 98%.

Cell Lines and Mouse Model

The rat Morris hepatoma cell line (MH3924A) and MH3924A stably transfected with the HSV-tk gene (MH3924A-stb-tk+) were utilized [12]. Cell lines were maintained in RPMI-1640 medium (Gibco, Invitrogen, Carlsbad, CA) supplemented with 20% fetal bovine serum at 37°C in a humidified incubator with 5% CO₂. Male CD-1 nu/nu mice (n=11/tracer), six to eight weeks old, weighing between 28–30 g were purchased from Charles River Laboratories (Wilmington, MA). All the experimental procedures using the animals were conducted according to protocols approved by the Animal Investigation Committee of Wayne State University. Mice were implanted subcutaneously with MH3924A and MH3924A-stb-tk+ cells (1×10^6 cells/100 μ l) in the right and left upper flanks, respectively. After inoculation, the tumor growth and animal weights were monitored three times a week. After two weeks, five and six animals were used for biodistribution for each tracer at 60 and 150 min respectively. Of the six mice from the 150 min group, three mice underwent dynamic microPET imaging prior to biodistribution.

Uptake studies

Both cell lines were seeded at 2×10^5 cell/ml in 6 well plates. After 48 hours, 50–60% confluent cells were incubated for two hours with either 37 kBq/mL of ³H-FAU or 1.85 kBq/mL of ¹⁴C-FIAU. At the end of the incubation period, radioactive medium was removed and wells were refreshed with non-radioactive medium for 10 min to remove any non-phosphorylated compound. Then, the effluxed activity was removed and the plates were rinsed three times with ice cold PBS. The trypsinized cells were solubilized using 0.2 ml of soluene-350, mixed with 5 ml of ultima gold scintillation cocktail and radioactivity measured for 5 minutes on a liquid scintillation counter (Tri-Carb, Packard Bioscience, Meriden, CT). Experiments were done in triplicate and external standard quench correction was used during beta isotope counting. Data were represented as percentage of incubated dose per 1×10^5 cells. To compare the selectivity between probes, accumulation ratios between HSV-TK and control cells for the same cell line (TK/control ratio) were calculated as a selectivity index [5].

Biodistribution Studies

Animals were injected with either ¹⁸F-FIAU or ¹⁸F-FAU (mean activity: 4.29 MBq; range: 3.51–5.99) in 200 μ l saline via a tail vein injection. At 60 (n=5) and 150 (n=6) min post injection the animals were sacrificed, selected tissues were harvested, weighed and activities were measured in a gamma spectrometer. If the tumor size was large, half the tumor was used to measure the radioactivity. The standard uptake values (SUVs) were calculated by dividing tissue radioactivity concentration (MBq/cc) by the injected radioactivity (MBq) per gram of body weight (assuming 1cc = 1gram) [13]. HPLC analysis of 60 min blood samples was performed to measure the metabolite concentration. For HPLC analysis, blood samples were processed mixing equal volumes of blood and 1M perchloric acid (PCA), vortexed, and centrifuged at 14,000 g for 3 minutes. The supernatants were analyzed by HPLC using a C-18 column (Hypersil ODS, 250 \times 4.6 mm) employing 10mM sodium acetate in 6% acetonitrile at a flow rate of 1 mL/minute.

In vivo Imaging

To determine the dynamic uptake of FIAU and FAU in the tumors, animals were injected with either ¹⁸F-FIAU or FAU (n=3 per tracer; mean activity: 4.29 MBq; range: 3.51–5.99) in 200 μ l saline via a tail vein injection. The animals were induced with 3% and maintained at 1.5% of isoflurane throughout the experiment. Anesthetized mice were placed in the microPET scanner (Concorde Microsystems R4, Knoxville, TN) in the supine position with the long axis of the animal parallel to the long axis of the scanner. With tumors near the

center of the field of view (CFOV) dynamic imaging was performed from 5 to 65 min post injection. At 65 and 120 min post injection, emission scans of 10 min duration with 2 overlapping frames were acquired to obtain a whole body image.

Image Analysis

The listmode data were first sorted into sinograms, Fourier rebinned and reconstructed using the ordered subset expectation maximization (OSEM 2D) algorithm. For reconstruction, a ramp filter was used with one half of the Nyquist frequency as the cut-off frequency. The dynamic image data were sorted into 21 frames with the time sequence: 9×60 s, 7×180 s, and 6×300 s. Circular Regions of Interest (ROIs) (~radius: 8 mm) covering the whole tumor were drawn on both the tumors to obtain the concentration of ^{18}F versus time. SUVs were calculated as described in the biodistribution section. The decay corrected time activity values were averaged over three animals.

Statistical analysis

Statistical Analysis of *in vitro* and *in vivo* studies was performed on Prism software (Graph pad, La Jolla, CA) using an unpaired, two-tailed t-test. *P*-values < 0.05 for the comparison between HSV-TK positive and corresponding controls were considered to be statistically significant.

RESULTS

Cell Incubation Studies

Incubation studies performed over a two hour time period demonstrated 34.5 (range: 27.4-39.7) and 25.5 (range: 24.8-26.5) fold higher accumulation of activity in the MH3924A-stb-tk+ expressing cell line compared to the control with FAU and FIAU respectively (Table 1). Even though the selectivity index of FAU is higher, the absolute accumulation is 100 fold less than that of FIAU suggesting a difference in phosphorylation by HSV-TK between the nucleosides.

Imaging and Biodistribution Studies with FIAU and FAU

In ^{18}F -FIAU injected mice, tumor volumes were 422 ± 164 and 472 ± 181 mm³ for MH3924A and MH3924A-stb-tk+ (*P*=0.57), respectively. Similarly, in ^{18}F -FAU injected mice tumor volumes were 419 ± 256 and 409 ± 170 for MH3924A and MH3924A-stb-tk+ (*P*=0.97), respectively. The whole body static images acquired at 65 and 120 min post injection show a clear accumulation of activity in MH3924A-stb-tk+ tumors in ^{18}F -FIAU injected animals (Figure 1). At both time points, activity in the control tumors was similar to that of muscle. Other organs with distinct contrast include gall bladder, kidneys and bladder, where activity is accumulated due to clearance of the tracer. Time activity curves generated from 5 min post injection for over 60 min show a continuous accumulation of activity in the MH3924A-stb-tk+ tumors. In the control MH3924A tumors, the SUV activity levels were less than one and reached a plateau within 10 min of tracer administration (Figure 2).

In the case of ^{18}F -FAU, even though uptake of activity was observed in the MH3924A-stb-tk+ tumors, the absolute accumulation SUV values were less than one (HSV-TK vs control *P*≤0.19). The time activity uptake of ^{18}F -FAU in the control MH3924A tumors was similar to that of ^{18}F -FIAU (Figure 2). Whole body images acquired from mice injected with ^{18}F -FIAU and ^{18}F -FAU is shown in Figure 1.

Biodistribution studies revealed, consistent with imaging, highest and significant uptake of activity in MH3924A-stb-tk+ tumors in ^{18}F -FIAU treated mice at both time points (HSV-TK vs control *P*≤0.007; Table 2 & Figure 3).

In ^{18}F -FAU injected mice, the MH3924A-stb-tk+ tumor ($\text{SUV} \pm \text{SE}$; 0.72 ± 0.09) activity was similar to that of control tumors (0.6 ± 0.07) and muscle (0.56 ± 0.05) at 60 min. At 150 min, there is a slight increase in accumulation of activity in the MH3924A-stb-tk+ tumor (1.01 ± 0.09), but non-significant to control tumor (0.73 ± 0.08), muscle (0.59 ± 0.07), kidneys (0.97 ± 0.06) and spleen (1.0 ± 0.09) (Table 2 & Figure 3). Blood activity levels at 60 and 150 min were less than that of tumors. At both time points, the activity in MH3924A-stb-tk+ tumors in ^{18}F -FIAU injected mice is two to four times higher than the FAU injected mice. The biodistribution of ^{18}F -FIAU and ^{18}F -FAU at both time points is presented in Table 2.

HPLC analysis of blood samples of ^{18}F -FIAU injected mice at 60 min showed 37% ($n=5$, range: 25–58%) of activity in its native form with the primary metabolite as ^{18}F -FAU. In ^{18}F -FAU injected mice, greater than 95% ($n=5$, range: 93–98%) of activity is its native form.

DISCUSSION

Several studies have demonstrated the use of radiolabeled FIAU for HSV-tk gene expression imaging [14, 15]. The primary interest for this study was to investigate the dynamic uptake and biodistribution of ^{18}F -FIAU and assess the substrate specificity of HSV-TK for FAU and contribution of ^{18}F -FAU formed during the HSV-tk gene expression imaging with ^{18}F -FIAU as a reporter probe. Toward this goal, a well characterized rat Morris hepatoma cell line stably expressing the HSV-tk gene (MH3924A-stb-tk+) under the CMV promoter was used for the experiments. The whole body images acquired at 65 and 120 min post injection show a clear and specific accumulation of activity in the HSV-TK expressing tumors. At both time points, the activity in the control tumors was similar to that of background activity.

The time activity curves acquired over 65 min show a continuous accumulation activity in the MH3924A-stb-tk+ tumor. This is in contrast to the radioiodinated analog where accumulation of activity was observed within the first 15 min but did not increase after that [16]. It is possible that, HSV-TK expression levels and specific activity of radiopharmaceutical may lead to such differences. The effect of tumor size was ruled out as there was no statistically significant difference in tumor volumes between the control and genetically modified tumors. In the control tumors, the activity retention was found to be reaching a plateau within 10 min and at all times the SUV was close to or less than one. These results suggest that there are significant differences in accumulation at 120 minutes which may be due to a significant difference in phosphorylation rates of these two nucleosides.

HPLC analysis of blood samples from the mice studies showed 37% of ^{18}F -FIAU in the native form. The primary metabolite was identified as ^{18}F -FAU, making up about 63% of the blood activity. To account for the contribution of ^{18}F -FAU generated by de-iodination of ^{18}F -FIAU to the total uptake seen in the MH3924A-stb-tk+ tumors, microPET imaging and biodistribution studies with ^{18}F -FAU were pursued.

Static images acquired at 65 min post injection of ^{18}F -FAU, showed uniform accumulation of activity through out the body other than kidneys, gall bladder and bladder. The MH3924A-stb-tk+ to MH3924A activity ratio was 1.18 suggesting no specific phosphorylation and retention due to HSV-TK phosphorylated species. This is supported by time activity curves over MH3924A-stb-tk+, which demonstrated a very slow accumulation of activity. Tissue analysis at 150 min showed a slight increase in MH3924A-stb-tk+ to MH3924A tumor activity ratio (1.45) in contrast to the cell culture uptake results, where the cells are continuously exposed to the substrate at an almost steady state concentration in

comparison to *in vivo*. The blood SUV values in ^{18}F -FAU injected mice at 60 and 150 min demonstrate less activity than both the tumors (Table 2). So it is unlikely that the observed uptake is because of high blood activity. However, one can rationalize the high ^{18}F -FAU uptake observed due to phosphorylation by mammalian TK, a hypothesis conceived for its development. On the other hand FIAU is a poor substrate to mammalian TK thus resulting in low background. Both these *in vitro* and *in vivo* results suggest that FAU is phosphorylated slowly in comparison to FIAU and there may be some transport differences between the nucleosides. This slow phosphorylation and accumulation of activity may be useful for therapeutic purposes since high levels of FAU can be maintained without much toxicity to normal tissue [17].

With ^{18}F -FAU as a probe, there is no significant difference in uptake was observed between the MH3924A-stb-tk+ and control tumors. Considering that FIAU is metabolized slowly with variable de-iodination rates, mice, dogs and humans at approximately 63%, 22%, and 1% (whole blood) [8, 18] at 60 min respectively, the contribution of FAU formed to the activity seen in MH3924A-stb-tk+ tumors with FIAU as an imaging agent is minimal. It is possible that FAU phosphorylation rates may also be different. For example, in cells expressing drosophila melanogaster deoxyribonucleoside kinase (Dm-dNK), reasonable FAU phosphorylation and accumulation of activity was demonstrated (Nimmagadda, unpublished data). This data suggests that the affinity of HSV-TK for FAU is minimal even if pure FAU is used as an agent under a robust promoter biological model. Recent clinical studies showed positive identification of bacterial infections within 2 hours post injection of ^{124}I -FIAU [7]. These short incubation times are very favorable and may expand the role of ^{18}F -FIAU for infection imaging. However, FAU substrate specificity to other viral and bacterial thymidine kinases needs to be addressed before utilizing ^{18}F -FIAU as an imaging agent for infection imaging.

This study demonstrates that ^{18}F -FIAU accumulates preferentially and continuously over 60 min in HSV-TK expressing tumors. Studies using ^{18}F -FAU did not reveal any specific uptake of activity in HSV-TK expressing tumors, making it an unsuitable agent to image suicide gene expression. The contribution ^{18}F -FAU formed to the total uptake seen in HSV-TK positive tumors in ^{18}F -FIAU injected mice is minimal.

Acknowledgments

The authors thank Mr. Kirk Douglas for assistance with HPLC and Drs. Otto Muzik and Xin Lu for microPET imaging support. This work is partially supported by grants from the National Cancer Institute, CA22453 and CA39566.

References

1. Macilwain C. Trial deaths prompt tighter rules. *Nature*. 1993; 366:294. [PubMed: 8247116]
2. Staschke KA, Colacino JM, Mabry TE, Jones CD. The *in vitro* anti-hepatitis B virus activity of FIAU [1-(2'-deoxy-2'-fluoro-1-beta-D-arabinofuranosyl-5-iodo)uracil] is selective, reversible, and determined, at least in part, by the host cell. *Antiviral Res*. 1994; 23:45–61. [PubMed: 8141592]
3. Tjuvajev JG, Finn R, Watanabe K, Joshi R, Oku T, Kennedy J, et al. Noninvasive imaging of herpes virus thymidine kinase gene transfer and expression: a potential method for monitoring clinical gene therapy. *Cancer Res*. 1996; 56:4087–95. [PubMed: 8797571]
4. Tjuvajev JG, Stockhammer G, Desai R, Uehara H, Watanabe K, Gansbacher B, et al. Imaging the expression of transfected genes *in vivo*. *Cancer Res*. 1995; 55:6126–32. [PubMed: 8521403]
5. Kang KW, Min JJ, Chen X, Gambhir SS. Comparison of $[^{14}\text{C}]$ FMAU, $[^3\text{H}]$ FEAU, $[^{14}\text{C}]$ FIAU, and $[^3\text{H}]$ PCV for monitoring reporter gene expression of wild type and mutant herpes simplex virus type 1 thymidine kinase in cell culture. *Mol Imaging Biol*. 2005; 7:296–303. [PubMed: 16041591]

6. Bettegowda C, Foss CA, Cheong I, Wang Y, Diaz L, Agrawal N, et al. Imaging bacterial infections with radiolabeled 1-(2'-deoxy-2'-fluoro-beta-D-arabinofuranosyl)-5-iodouracil. *Proc Natl Acad Sci U S A*. 2005; 102:1145–50. [PubMed: 15653773]
7. Diaz LA, Foss CA, Thornton K, Nimmagadda S, Endres CJ, Uzuner O, et al. Imaging of Musculoskeletal Bacterial Infections by [I]FIAU-PET/CT. *PLoS ONE*. 2007; 2:e1007. [PubMed: 17925855]
8. Nimmagadda S, Mangner TJ, Douglas KA, Muzik O, Shields AF. Biodistribution, PET, and radiation dosimetry estimates of HSV-tk gene expression imaging agent 1-(2'-Deoxy-2'-18F-Fluoro-beta-D-arabinofuranosyl)-5-iodouracil in normal dogs. *J Nucl Med*. 2007; 48:655–60. [PubMed: 17401105]
9. Collins JM, Klecker RW, Katki AG. Suicide prodrugs activated by thymidylate synthase: rationale for treatment and noninvasive imaging of tumors with deoxyuridine analogues. *Clin Cancer Res*. 1999; 5:1976–81. [PubMed: 10473074]
10. Sun H, Collins JM, Mangner TJ, Muzik O, Shields AF. Imaging [(18F)FAU [1-(2'-deoxy-2'-fluoro-beta-D-arabinofuranosyl) uracil] in dogs. *Nucl Med Biol*. 2003; 30:25–30. [PubMed: 12493539]
11. Mangner TJ, Klecker RW, Anderson L, Shields AF. Synthesis of 2'-deoxy-2'-[18F]fluoro-beta-D-arabinofuranosyl nucleosides, [18F]FAU, [18F]FMAU, [18F]FBAU and [18F]FIAU, as potential PET agents for imaging cellular proliferation. Synthesis of [18F]labelled FAU, FMAU, FBAU, FIAU. *Nucl Med Biol*. 2003; 30:215–24. [PubMed: 12745012]
12. Haberkorn U, Altmann A, Morr I, Knopf KW, Germann C, Haeckel R, et al. Monitoring gene therapy with herpes simplex virus thymidine kinase in hepatoma cells: uptake of specific substrates. *J Nucl Med*. 1997; 38:287–94. [PubMed: 9025757]
13. Nimmagadda S, Mangner TJ, Sun H, Klecker RW Jr, Muzik O, Lawhorn-Crews JM, et al. Biodistribution and Radiation Dosimetry Estimates of 1-(2'-Deoxy-2'-18F-Fluoro-1-{beta}-D-Arabinofuranosyl)-5-Bromouracil: PET Imaging Studies in Dogs. *J Nucl Med*. 2005; 46:1916–22. [PubMed: 16269607]
14. Tjuvajev JG, Avril N, Oku T, Sasajima T, Miyagawa T, Joshi R, et al. Imaging herpes virus thymidine kinase gene transfer and expression by positron emission tomography. *Cancer Res*. 1998; 58:4333–41. [PubMed: 9766661]
15. Alauddin MM, Shahinian A, Park R, Tohme M, Fissekis JD, Conti PS. In vivo evaluation of 2'-deoxy-2'-[(18F)fluoro-5-iodo-1-beta-D-arabinofuranosyluracil ([18F]FIAU) and 2'-deoxy-2'-[18F]fluoro-5-ethyl-1-beta-D-arabinofuranosyluracil ([18F]FEAU) as markers for suicide gene expression. *Eur J Nucl Med Mol Imaging*. 2007; 34:822–9. [PubMed: 17206416]
16. Tjuvajev JG, Doubrovin M, Akhurst T, Cai S, Balatoni J, Alauddin MM, et al. Comparison of radiolabeled nucleoside probes (FIAU, FHBG, and FHPG) for PET imaging of HSV1-tk gene expression. *J Nucl Med*. 2002; 43:1072–83. [PubMed: 12163634]
17. Lin T, Chang C, Noker P, Smith A, Page J. Disposition of 2'-fluoro-ara-deoxyuridine (FAU, NSC-678515) in beagle dogs. *Proc Am Assoc Cancer Res*. 2000:703.
18. Vaidyanathan G, Zalutsky MR. Preparation of 5-[131I]iodo- and 5-[211At]astato-1-(2-deoxy-2-fluoro-beta-D-arabinofuranosyl) uracil by a halodestannylation reaction. *Nucl Med Biol*. 1998; 25:487–96. [PubMed: 9720667]

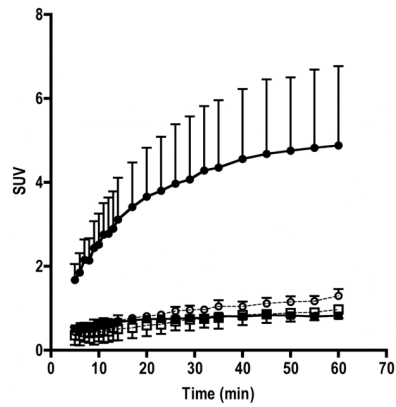


Fig 1. HSV-tk gene expression imaging with ^{18}F -FIAU and ^{18}F -FAU

Representative coronal images of mice bearing MH3924A-stb-tk+ (Left flank, arrows) and MH3924A (Right flank, circles) tumors injected with ^{18}F -FIAU (panels a and b) or ^{18}F -FAU (panels c and d) at 65 (Panels a and c) and 120 min (panel c and d) post-injection, respectively.

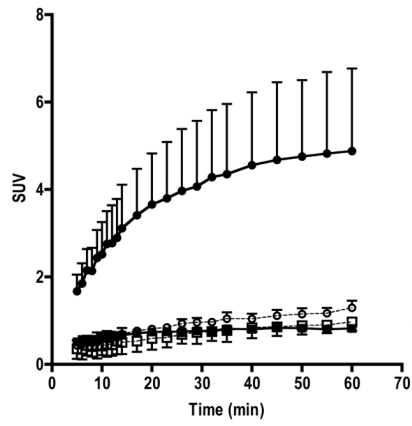


Fig 2. Time activity curves of ^{18}F -FIAU and ^{18}F -FAU retention in MH3924A-stb-tk+ and MH3924A control tumors

The activity curves shown are mean+SD values (n=3). ◆ FIAU MH3924A; ● FIAU MH3924A-stb-tk+ ; ◇ FAU MH3924A; ○ FAU MH3924A-stb-tk+

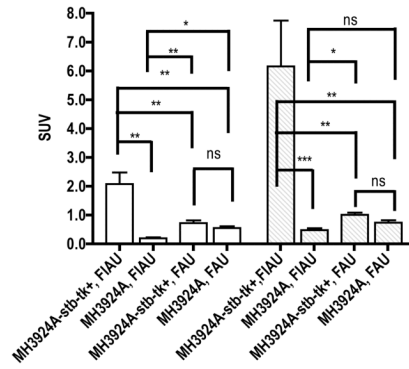


Fig 3. Comparison of ^{18}F -FIAU and ^{18}F -FAU accumulation in HSV-TK expressing and control tumors at 60 and 150 min post injection

All the activity values from ex vivo counting were converted into standard uptake values.

Values are mean \pm standard error (n=5). NS, nonsignificant, * $P < 0.05$, ** $P < 0.01$, *** $P < 0.001$

Table 1
Intracellular accumulation of ^{14}C -FIAU and ^3H -FAU in HSV-tk expressing and control MH3924A cells grown in culture

Cell retention measured as percent of incubated dose/ 10^5 cells and converted into selectivity index.

	MH3924A	MH3924A-stb-tk+	Selectivity index	P value
	% of incubated dose/ 10^5 cells			
FIAU	0.285	7.261	25.5	<0.0001
FAU	0.002	0.075	34.5	<0.0001

Table 2
Biodistribution of [¹⁸F]FIAU and [¹⁸F]FAU at 60 and 150 minutes post injection in CD1 nu/nu mice harboring HSV-TK positive tumors

All the activity values from ex vivo counting were converted to standard uptake values and expressed as mean \pm standard error (n=5 or 6).

	[¹⁸ F]FIAU		[¹⁸ F]FAU	
	60 min	150 min	60 min	150 min
Blood	0.03 \pm 0.01	0.04 \pm 0.02	0.22 \pm 0.14	0.14 \pm 0.05
Muscle	0.12 \pm 0.02	0.25 \pm 0.06	0.56 \pm 0.05	0.59 \pm 0.07
Lungs	0.30 \pm 0.12	0.27 \pm 0.08	0.36 \pm 0.03	0.40 \pm 0.02
Heart	0.21 \pm 0.05	0.39 \pm 0.11	0.62 \pm 0.10	0.67 \pm 0.12
Liver	0.24 \pm 0.07	0.50 \pm 0.19	0.67 \pm 0.06	0.68 \pm 0.04
Spleen	0.22 \pm 0.05	0.46 \pm 0.10	0.98 \pm 0.12	1.10 \pm 0.09
Intestine	0.13 \pm 0.02	0.32 \pm 0.10	0.36 \pm 0.05	0.40 \pm 0.03
Kidney	0.69 \pm 0.20	0.96 \pm 0.37	1.02 \pm 0.11	0.97 \pm 0.06
Stomach	0.08 \pm 0.02	0.14 \pm 0.04	0.35 \pm 0.05	0.32 \pm 0.03
Femur	0.09 \pm 0.02	0.24 \pm 0.07	0.40 \pm 0.06	0.44 \pm 0.03
MH3924A-stb-tk+	2.07 \pm 0.40	6.15 \pm 1.58	0.72 \pm 0.09	1.01 \pm 0.07
MH3924A	0.19 \pm 0.07	0.47 \pm 0.06	0.60 \pm 0.06	0.73 \pm 0.08